E3-2009-183

S. A. Karamian, J. J. Carroll*

CROSS SECTION FOR INELASTIC NEUTRON ACCELERATION BY ^{178}Hf^{m2}

Submitted to «ECT Workshop on Atomic Effects in Nuclear Excitation and Decay», June 15–19, 2009, Trento, Italy

*Department of Physics and Astronomy, Youngstown State University, Youngstown, Ohio, USA

Карамян С. А., Кэрролл Дж. Дж. E3-2009-183

Сечение неупругого ускорения нейтронов изомером $^{178}\mathrm{Hf}^{m2}$

При рассеянии тепловых нейтронов изомерными ядрами в некоторых случаях энергия выходящего нейтрона может возрасти. Этот процесс получил название неупругого ускорения нейтронов (INNA), при котором ядро в конечном состоянии после эмиссии нейтрона остается с меньшей энергией, чем энергия возбуждения изомера. В результате происходит вынужденная разрядка изомера с заселением основного состояния. Эмиссия нейтрона должна сопровождаться каскадным испусканием нескольких гамма-квантов, чтобы унести высокий угловой момент исходного изомерного состояния. В нескольких случаях ранее процесс INNA был зафиксирован, но хорошего соответствия с теоретическими оценками сечения не было достигнуто. Недавние измерения сечения INNA дали результат $\sigma_{\mathrm{INNA}} = (258 \pm 58)$ б для рассеяния нейтронов на $^{177}\mathrm{Lu}^{m}$. В настоящей работе $\sigma_{\mathrm{INNA}} = 152^{+51}_{-36}$ б получено на основе измерения полного сечения «сжигания» изомера $^{178}\mathrm{Hf}^{m2}$ при облучении тепловыми нейтронами. Данный изомер отличается высоким спином и четырехквазичастичной структурой. В анализе использованы статистические оценки вероятности различных каналов реакции после поглощения нейтрона. Полученное значение σ_{INNA} сравнивается с теоретически предсказанным сечением.

Работа выполнена в Лаборатории ядерных реакций им. Г. Н. Флерова ОИЯИ.

Препринт Объединенного института ядерных исследований. Дубна, 2009

Karamian S. A., Carroll J. J. E3-2009-183

Cross Section for Inelastic Neutron Acceleration by $^{178}\mathrm{Hf}^{m2}$

The scattering of thermal neutrons from isomeric nuclei may include events in which the outgoing neutrons have increased kinetic energy. This process has been called Inelastic Neutron Acceleration (INNA) and occurs when the final nucleus after emission of the neutron is left in a state with lower energy than that of the isomer. The result, therefore, is an induced depletion of the isomeric population to the ground state. A cascade of several gammas must accompany the neutron emission to release the high angular momentum of the initial isomeric state. INNA was previously observed in a few cases and the associated cross sections were only in modest agreement with theoretical estimates. The most recent measurement of an INNA cross section was $\sigma_{\mathrm{INNA}} = (258 \pm 58)$ b for neutron scattering by $^{177}\mathrm{Lu}^{m}$. In the present work, an INNA cross section of $\sigma_{\mathrm{INNA}} = 152\,^{+51}_{-36}$ b was deduced from measurements of the total burn-up of the high-spin, four-quasiparticle isomer $^{178}\mathrm{Hf}^{m2}$ during irradiation by thermal neutrons. Statistical estimates for the probability of different reaction channels past neutron absorption were used in the analysis, and the deduced σ_{INNA} is compared to the theoretically predicted cross section.

The investigation has been performed at the Flerov Laboratory of Nuclear Reactions, JINR.

Preprint of the Joint Institute for Nuclear Research. Dubna, 2009

INTRODUCTION

In 1959 it was suggested [1] that neutron scattering from nuclei entirely in an excited state, such as an isomer, could include reactions in which neutrons were «accelerated» by the interaction.* The higher energy of the outgoing neutron would result from the transfer of some excitation energy from a target nucleus, leaving the final nucleus in a state of lower energy. This process was called an INelastic Neutron Acceleration, or INNA, reaction (the term *superelastic scattering* is sometimes used as well) and was proposed to be interesting not only from a purely physical perspective, but also in view of possible applications based on an induced release of energy stored in long-lived isomers. A few experiments were made [3–6] and evidence of the effect was reported in [5, 6] with associated cross-section values. In general, experiments can be expected to be difficult. One factor is that the cross sections may be reduced by nuclear structure hindrances, which could play a role in this reaction, in addition to the effects of selection rules for angular momentum and parity. Also, successful direct detection of the accelerated neutrons is difficult using standard methods of neutron spectrometry due to the intense flux of fast neutrons near a reactor. Nevertheless, it is clear that the INNA reaction due to scattering from nuclear isomers should be possible at some level and worthy of study. It should be noted that the cross section for superelastic proton scattering from a nuclear isomer was discussed in [7]. Similar processes are also known in other physical domains, e.g., in atomic collisions or in scattering of ultracold neutrons from condensed matter, where thermal excitation energy of a system can be transferred into kinetic energy of a scattered projectile. The probability of this exchange is related to the great phase volume of phonon modes in solids, unlike for INNA from isomers where few nuclear levels are available for the final state of the reaction.

The interaction of external radiation with high-spin isomers like $^{178}\mathrm{Hf}^{m2}$ and $^{177}\mathrm{Lu}^{m}$ has been of particular interest (see [8–10] and references therein) and thermal neutron reactions with $^{177}\mathrm{Lu}^{m}$ $(23/2^{-})$ were recently explored using an activation method [11]. A relatively high cross section of $\sigma_{\mathrm{INNA}} = 258 \pm 58$ b

*The process discussed herein differs from acceleration of neutrons by magnetic fields, as described in [2].

was deduced for INNA by the isomer, a value much larger than the theoretical estimate described in that work. Independently and at nearly the same time, a similar method was used at the Joint Institute for Nuclear Research, Dubna (Russia) to study the production, σ_p, and burn-up, σ_b, cross sections for $^{178}\mathrm{Hf}^{m2}$ (16^+) due to reactor neutrons [12]. Metal Hf samples of natural composition were exposed to the neutron flux from the IBR-2 reactor and the induced activities of various daughters were studied. Irradiations of the samples were performed in different shielding conditions and with varied fluences. A surprisingly large thermal cross section of $\sigma_b = 235 \pm 30$ b was deduced for burn-up of this high-spin isomer, with a significant part of that value being tentatively attributed to the (n, γ) reaction branch populating the ^{179}Hf ground state. In the present work, an estimate is made of the portion of this burn-up cross section that is due to inelastic neutron acceleration by the K-hindered, long-lived, four-quasiparticle isomer of ^{178}Hf. A comparison is made between this value and the results obtained for $^{177}\mathrm{Lu}^m$ and earlier experiments [5, 6, 11, 13] to establish a systematic description for this process.

1. ISOMER-TO-GROUND STATE RATIO VIA MODEL ESTIMATES

The burn-up cross section for a medium weight nucleus may be expressed as the sum

$$\sigma_b = \sigma_{\mathrm{INNA}} + \sigma_m + \sigma_g, \tag{1}$$

where σ_m and σ_g correspond to the population of isomeric and ground states, respectively, in the daughter nucleus produced by radiative capture. In Eq. (1), only three inelastic processes are represented since elastic scattering cannot contribute to σ_b. Also, it is assumed that the cross sections for neutron-induced fission and the (n, α) reaction are negligible for the nucleus of interest. Finally, the daughter ^{179}Hf possesses two isomers with half-lives of 18.67 s ($m1$) and 25.05 d ($m2$). Due to its short half-life, population of $^{179}\mathrm{Hf}^{m1}$ after neutron capture on $^{178}\mathrm{Hf}^{m2}$ is considered herein to contribute to the ground state of ^{179}Hf (and thus to σ_g). The cross section for the branch of the (n, γ) reaction populating the $^{179}\mathrm{Hf}^{m2}$ (25/2$^-$) isomer from $^{178}\mathrm{Hf}^{m2}$ was previously measured to be $\sigma_m = 45 \pm 5$ b [14, 15]. Equation (1) can then be used to determine the portion of the burn-up due to inelastic neutron acceleration, σ_{INNA}, based on the experimental result for σ_b [12] and once a value of σ_g is known. The latter value can be determined using the measured σ_m and an estimated isomer-to-ground state ratio, σ_m/σ_g.

Semi-empirical systematics for isomer-to-ground state ratios have been discussed in the literature and theoretical approaches have also been developed. The treatment of Huizenga and Vandenbosch [16] is still valid: the ratio is defined by the gamma cascade that occurs in the excited residual nucleus past particle emission. The isomer-to-ground state ratio is then a consequence of the properties of the cascades that populate either the ground state or the isomer. The initial distributions of angular momentum and excitation energy after absorption of a particle crucially influence the paths to these final states, but the position of low-lying levels may also affect the σ_m/σ_g ratio. This reaction model has been applied for decades to results obtained in two different domains, namely: in reactions with light projectiles, photons and neutrons with low spin of the reaction product; and in reactions with heavy ions, when a maximum angular momentum as high as $I_{\max} = 30 - 50$ can be released. The gamma cascade paths are very different in these two cases. After thermal neutron absorption, the compound nucleus typically emits a cascade of 2–3 gammas to reach lower-lying excited states with $I \leqslant 4$, proceeding then to the ground state. This is because the reaction residue is located far from the yrast line in the standard (E^*, I) diagram. Having low angular momentum and considerable excitation energy, the nucleus emits statistical quanta of $E1$ multipolarity with mean energies near 1.5–2 MeV. High-spin isomers with $I > 6$ are, therefore, populated with a low probability on the order of 10^{-3}–10^{-5} which varies among different nuclides.

In a heavy-ion induced fusion-evaporation reaction, the compound nucleus also emits a few quanta of statistical nature at the initial stage of the cascade. Then the cascade trajectory approaches and proceeds along the yrast line. Emission by multiple stretched gamma transmissions, typically of $E2$ multipolarity, drives the cascade through the collective ground-state band and other rotational bands built on the lowest-lying vibrational and intrinsic levels. This high-multiplicity cascade serves to remove the excess angular momentum, and the population of high-spin isomers is also useful for that. Nevertheless, typical σ_m/σ_g values only reach 0.1–1.0, because the spin distribution of the heavy-ion induced compound nucleus is wide and extends from 0 to $I_{\max}$. Even for high values of $I_{\max}$, products with low angular momenta exist in the initial spin distribution. This supplies a significant cross section for population of the low-spin ground state, bypassing high-spin isomers.

It should be stressed that reactions in which a high-spin isomer serves as a target or as a projectile permit access to an unusual third domain for reaction products in the (E^*, I) diagram. The excitation energy reached via neutron absorption by an isomeric target is comparable or even a little higher than that achieved in $(n,\ \gamma)$ reactions on ground state targets. However, the resulting compound nucleus spin, I, is much larger when using isomeric targets of high spin (although I may not reach as large an $I_{\max}$ as in heavy-ion reactions) yet exhibits a narrow distribution of values at $I = I_m \pm 1/2$. Thus, high-spin isomers should be abundantly populated in the results of $(n,\ \gamma)$ reactions on isomers, and the σ_m/σ_g values may even exceed those observed for fusion-evaporation products with heavy projectiles. Evidence of this behavior was obtained in a series of experiments with isomeric $^{178}\mathrm{Hf}^{m2}$ and $^{180}\mathrm{Ta}^{m}$ targets [17].

In accordance with these ideas, Fig. 1 depicts in schematic fashion the feeding of the $^{179}\mathrm{Hf}^{m2}$ isomer in the residual nucleus following the $^{178}\mathrm{Hf}^{m2}$ $(n,\ \gamma)$ reaction. The emphasis is on the stretched cascades which occur after statistical gamma emission and is in agreement with the well-established model of [16]. The full level scheme [18] contains many more bands than are shown in Fig. 1, most of which do not significantly feed $^{179}\mathrm{Hf}^{m2}$ as discussed later. Thermal neutron absorption populates $31/2^{+}$ and $33/2^{+}$ resonances located at $E^{*} = 8.545$ MeV. Then a cascade of 2–3 $E1$ quanta is emitted since the excitation energy is rather high above the yrast line so that the states involved in the cascade are defined only by statistical properties of gamma emission, not by collective band structure. This phase is similar to that in the standard $(n,\ \gamma)$ reaction mechanism known for low-spin stable targets and does not yet define which final state (isomer or ground) will be populated. The following phase, however, more closely resembles the cascade pattern typical for heavy-ion induced reactions, because collective bands near the yrast line should be populated at spins corresponding to this discussion.

The statistical quanta reduce E^{*} without significant change in the angular momentum due to the essentially random orientation of the photon spin, as follows from level density estimations. One can then isolate a range in (E^{*}, I) that serves as an intermediate stage for the population of bands built on either the ground state or the $m2$, $25/2^{-}$ isomer. The intermediate state range is shown in Fig. 1 by the dashed-line box near 2.5 MeV. The cascade path should follow near the yrast line because of definite excess of the angular momentum. The 25/2^{-} isomeric band just serves as the yrast one in the corresponding range of E^{*}. Thus, the $m2$ isomer could not be passed by without population. In the works [12, 15], the $m1$ population was not isolated as an independent process and it was included in the strength that finally reaches the ground state. The band structure at high spin is given in accordance with results of in-beam gamma spectroscopy [19].

It is possible to draw some conclusions concerning the σ_m/σ_g ratio from the scheme shown in Fig. 1. A stretched 3-fold $E1$ cascade is necessary to feed the $25/2^{-}$ level in the $m2$ band from the $31/2^{+}$ intermediate state, as well being necessary to feed the $27/2^{-}$ level of the $m2$ band from the $33/2^{+}$ intermediate state. A cascade multiplicity $M_{\gamma} = 2$ is forbidden by the parity selection rule.* Similarly, the ground-state band can be populated via 4-fold dipole cascades to levels of comparable spin located a little higher in energy than those in the isomer band. Smaller multiplicity cascades of $M_{\gamma} = 3$ are again forbidden by parity.

Feeding of the $m1$ band requires much higher multiplicity of stretched cascades and the feeding probability is thereby greatly reduced; the $m1$ band is, therefore, eliminated from the following discussion. What then can be deduced

*Non-parity-conserving transitions are not considered herein.

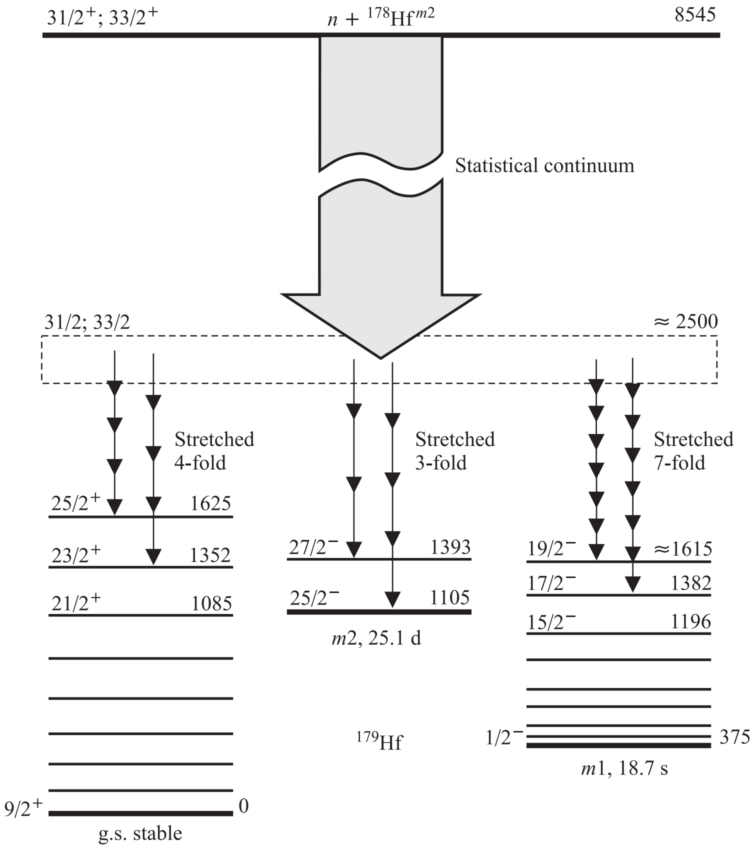

Fig. 1. Partial level scheme modeling the $^{178}\mathrm{Hf}^{m2}(n,\,\gamma)$ reaction, emphasizing stretched gamma cascades leading to population of the ground and isomeric states in ^{179}Hf. The focus on a limited number of states and transitions after statistical dipole cascade is consistent with the model of [16] and no attempt is made to give a full level diagram. Level energies are given in keV

from a comparison between the cascades going to the ground state and $m2$ bands? The photon spin emitted in a dipole transition may have three different orientations relative to the initial direction of the nuclear spin. Each spin projection for the emitted photon will then exist with a probability of about 1/3. A stretched cascade of definite orientation is needed to decrease the nuclear spin regularly by unity at each step from the intermediate state spin to that of the indicated band members. The progression must follow $I \to (I-1) \to (I-2) \to (I-3)$ and the statistical probability of such a cascade is estimated to be about $(1/3)^{M_\gamma}$.

Consequently, a 4-fold stretched cascade is characterized by a probability that is 1/3 of that of a 3-fold stretched cascade. From the scheme shown in Fig. 1, the conclusion follows that simply due to the statistical reasons, population of the $m2$ isomer in ^{179}Hf should be three times more probable than population of the ground state, with $\sigma_m/\sigma_g = 3$.

In the above estimate, two difficulties may be considered: a) why was $E1$ multipolarity chosen for the feeding transitions, and b) what would be the result if negative parity was assumed for the intermediate states? It is known that generally the strength of $E1$ electromagnetic transitions is larger than that of higher-multipolarity transitions. The $E2$ and $M1$ multipolarities dominate only for transitions within collective bands, while for statistical quanta $E1$ is normally assumed. For the second point, if one assumes negative parity for the intermediate states, this will allow 2-fold stretched cascades for population of the $m2$ isomer and 3-fold stretched cascades for population of the ground-state band. In this case, a factor 3 characterizing the preferential feeding of the isomer arises again. This conclusion is insensitive to the parity of the intermediate states.

The population of the $m2$ state in ^{179}Hf following the $^{178}\mathrm{Hf}^{m2}(n,\gamma)$ reaction may also be assessed based on a different model involving level density estimates. Suppose the compound nucleus resonances decay at the first step of gamma emission into two «independent» families of levels that channel separately into either the isomer or the ground state. The decision as to the identity of the final state (isomer or ground) is then defined much earlier past compound nucleus formation than in the previous model of stretched gamma cascades near the yrast line. The relative probability for the two channels would be defined by the ratio of level densities for the families of states: that bound to the ground state, designated by G; and that bound to the isomer, designated by M. One can estimate this ratio using the spin-dependent level density $\rho(E^*, I)$ according to the Gilbert–Cameron equation [20]:

$$\rho(E^*, I) = \frac{(2I+1)\exp\left[2\sqrt{aE^*} - (I+1/2)^2/2\sigma^2\right]}{24\sqrt{2}a^{1/4}(E^*)^{5/4}\sigma^3}, \tag{2}$$

where $a = A/10$ is the level density parameter and $\sigma^2 = 0.0888A^{2/3}a^{1/2}(E^*)^{1/2}$. For family G, real E^* and I values of the compound resonances shown in Fig. 1 were assumed. For the isomeric family M, the parameters are taken to be $E^*_M = E^* - E_m$ and $I_M = I - I_m$, where E_m and I_m correspond to the isomer itself. The emitted photon energy $E_\gamma = 1.5$ MeV is assumed as typical for the statistical cascade. The resulting estimate of $\sigma_m/\sigma_g = 2.2$ compares well to the value predicted above with the stretched cascade scheme, despite the different assumptions.

In both approaches to an estimate of the isomer-to-ground-state ratio, an important factor was ignored. In reality, there exists a variety of cascade trajectories through bands which feed the $m2$ and ground states and the actual pattern is not as simple as was described above. Fourteen bands have been identified [18] for ^{179}Hf. Once a cascade has begun within one of these bands, the predominance of collective intra-band transitions will most often lead to the respective bandheads, which are typically of lower spin than $^{179}\mathrm{Hf}^{m2}$. From most bands, one can therefore expect only weak population of the $m2$ isomer by competing inter-band transitions high above the bandheads. However, 5 high-spin bands have been found [19], populated by incomplete fusion reactions and detected by in-beam gamma spectroscopy, that provide measurable feeding of the $m2$ isomer from their bandheads. It may be expected, therefore, that the fraction of bands in ^{179}Hf that are presently known to populate the isomer (0.36) serves as a lower limit on the isomer-to-ground-state ratio σ_m/σ_g resulting after neutron capture by $^{178}\mathrm{Hf}^{m2}$. After all, the compound nucleus will be populated at high spin (since the capturing nucleus is in the $I^\pi = 16^+$ $^{178}\mathrm{Hf}^{m2}$ state), and this will emphasize population of the high-spin bands whose bandheads feed $^{179}\mathrm{Hf}^{m2}$.

Specifics of band structure are unique for each nuclide and this creates an additional factor to be considered in the evaluation of σ_m/σ_g beyond statistical arguments. For instance, the 9^- isomeric level in ^{178}Lu is located at just 120 keV, so that the isomer band is yrast down to the lowest energies. Therefore, almost the full strength of the gamma cascades may be collected by the isomeric band, as is reflected in a high σ_m/σ_g for ^{178}Lu [13, 17]. The level scheme of ^{179}Hf is quite different, and estimates of the isomer-to-ground-state ratio which are correct for this nuclide are not necessarily valid for ^{178}Lu. This is despite the fact that target nuclei of $^{178}\mathrm{Hf}^{m2}$ and $^{177}\mathrm{Lu}^{m}$ are both examples of multi-quasiparticle, K-hindered isomers.

2. RESULTS AND DISCUSSION

Additional information on the magnitude of σ_m/σ_g for the $^{178}\mathrm{Hf}^{m2}(n,\gamma)$ reaction can be obtained by direct comparison to systematics from available experimental data for other reactions. Table 1 collects the relevant values from various measurements. Some experiments shown in the table are special, utilizing isomeric targets of $^{180}\mathrm{Ta}^{m}$ and $^{178}\mathrm{Hf}^{m2}$ [17, 21], and are similar to that expected here, with a narrow spin distribution concentrated near the high spin of the target nucleus. Other reactions in Table 1 provide isomer-to-ground-state ratios obtained for production of $^{179}\mathrm{Hf}^{m2}$ and other isomers of similar structure in Lu and Hf nuclides [19, 22]. Figure 2 displays the measured isomer-to-ground-state ratios as a function of spin deficit $\Delta I = I_m – I_r$ in the reactions, where I_m is the final isomer spin and I_r is the residue after the reaction.

It can be seen in Fig. 2 that the isomer-to-ground state ratios show systematic trends based on two parameters: the spin deficit in the reaction and the excitation

Table 1. Isomer-to-ground state ratios measured with typical experimental errors of 20%

Reaction and reference	Target spin	Spin distribution		Product isomer	Isomer spin I_m	Isomer energy E_m, MeV	$\frac{\sigma_m}{\sigma_g}$
		Descr.	Mean I				
^{176}Yb(^{9}Be, $\alpha 2n$) [19]	0	Wide	≈ 13	^{179}Hf^{m2}	25/2	1105.74	0.13*
^{176}Yb(^{4}He, n) [22]	0	Wide	11	^{179}Hf^{m2}	25/2	1105.74	0.08
^{176}Yb(^{4}He, $2n$) [22]	0	Wide	11	^{178}Hf^{m2}	16	2446.09	0.05
^{176}Yb(^{4}He, $p2n$) [22]	0	Wide	9	^{177}Lu^{m}	23/2	970.175	0.05
^{179}Hf(γ, p) [17]	9/2	Narrow	6 ± 2	^{178}Lu^{m}	9	123.8	0.55**
^{180}Ta^{m} (n, $n\prime$) [21]	9	Narrow	9 ± 2	^{180}Ta^{m}	9	77.1	1.5
^{180}Ta^{m} (γ, p) [17]	9	Narrow	8 ± 2	^{179}Hf^{m2}	25/2	1105.74	0.09
^{180}Ta^{m} (γ, $2n$) [17]	9	Narrow	9 ± 3	^{178}Ta^{m}	7	~ 0	3
^{178}Hf^{m2} (γ, n) [17]	16	Narrow	16 ± 2	^{177}Hf^{m2}	37/2	2740.02	0.12

*Evaluated from gamma intensities [19] and accounting for electron conversion.
**Corrected using currently accepted gamma intensities in decay of ^{178}Lu.

energy of the final isomeric state. For the reactions having wide spin distributions, the product isomers are also of high energy, lying near or above 1 MeV. Their isomer-to-ground-state ratios are significantly less than 1, suppressed both by a compressed energy space in which gamma cascades must populate the isomer from the reaction residue and by the wide residual spin distribution. A high-spin isomer at low energy may serve as an yrast trap, utilizing a gamma cascade over nearly the full residual excitation energy of the nucleus. The increase in isomer-to-ground-state ratios with decreasing spin deficit was previously found in [17] and in accordance with model expectations.

On the other hand, reaction residues with narrow spin distributions in Fig. 2 contain measurements with both cases of E_m near or greater than 1 MeV and E_m at low energies (less than 200 keV). The observed enhancement of the isomer-to-ground-state ratio is now clear for product isomers of low excitation energy as compared with product isomers of high excitation energy. Essentially, a high-spin isomer at low energy may serve as an yrast trap, reached by a gamma cascade that spans nearly the full excitation energy of the residual nucleus. The general trend for those measurements suggests a value of $\sigma_m/\sigma_g \sim 1$ for the $E_m = 1105$ keV isomer ^{179}Hf^{m2} when produced with a spin deficit -3.5 (in reality, a spin excess) in the ^{178}Hf^{m2} (n, γ) reaction. Being the ^{179}Hf^{m2} isomer located at low energy, the isomer-to-ground state ratio would be even larger.

The model estimates of σ_m/σ_g are 3, 2.2 and 0.36 (as a lower limit), while the experimental results plotted in Fig. 2 suggest a value near 1. The scattering

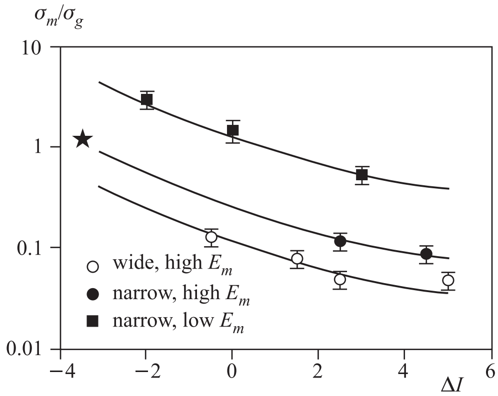

Fig. 2. Measured isomer-to-ground state ratios from Table 1 plotted as a function of the spin deficit for the producing reaction. Reactions characterized by narrow spin distributions in the reaction residue have filled symbols and wide spin distributions have open symbols. Circles indicate that the final isomeric state is near or above 1 MeV, and squares indicate final isomeric states of low energy, being less than 200 keV. The curves are provided to guide the eye and the starred point shows the composite isomer-to-ground-state ratio deduced for the $^{178}\mathrm{Hf}^{m2}(n,\gamma)^{179}\mathrm{Hf}^{m2}$ reaction, having a spin deficit of -3.5

of values suggested the use of a geometric mean and the value deduced from the measurements was given twice the weight of the model estimates since the former should be more reliable. The final composite estimate is $\sigma_m/\sigma_g = 1.2^{+1.0}_{-0.6}$. Using this isomer-to-ground-state ratio and the measured $\sigma_m = 45\ \pm 5$ b [14, 15], the cross section for ground-state population was found to be $\sigma_g = 38^{+41}_{-19}$ b. The cross section for inelastic neutron acceleration from $^{178}\mathrm{Hf}^{m2}$ was then determined from Eq. (1):

$$\sigma_{\mathrm{INNA}} = 152^{+51}_{-36}\ \mathrm{b}. \tag{3}$$

Propagation of only the measurement errors in σ_m and σ_b would have given an uncertainty in Eq. (3) near the 20% level typical in the works [5, 6, 11], where the INNA cross section was successfully measured for other isomers. The remaining uncertainty in Eq. (3) arises from the estimate of the isomer-to-ground-state ratio for this first determination of σ_{INNA} for the exotic $^{178}\mathrm{Hf}^{m2}$ isomer.

The value given in Eq. (3) may be compared to theoretical predictions for inelastic neutron acceleration by $^{178}\mathrm{Hf}^{m2}$. Following the approach of [11, 23], the cross section for this process is

$$\sigma_{\mathrm{INNA}} = 0.404 \cdot 10^8 \left(\frac{A+1}{A}\right)^2 g(I) S_0^2 \frac{T_\ell(E_n)}{T_0(E_0)}\ \text{barn}, \tag{4}$$

where $g(I)$ is the statistical spin factor, S_0 and $T_0(E_0)$ are the strength function and transmission coefficient for s-wave neutrons of thermal energy, and $T_l(E_n)$

is the transmission coefficient corresponding to the energy and orbital angular momentum of the accelerated neutron. The latter factor plays a crucial role in determining σ_{INNA} for specific isomer and daughter levels. Therefore, it is necessary to define which levels may be effective for the neutron acceleration past inelastic scattering from $^{178}\mathrm{Hf}^{m2}$.

A partial level scheme for ^{178}Hf is shown in Fig. 3, where the selected states are lower in energy than the $m2$, 16^{+} isomer [24]. Among all lower-lying states, only those of the highest angular momentum are relevant here. Reactions leading to lower-spin levels require high orbital momentum of the scattered neutron with a corresponding T_l that is drastically decreased in magnitude. Clearly, depletion of the 16^{+} isomer to levels with spins lower than 11 is practically forbidden by the centrifugal barrier manifested in the T_l values. The energy gain of the neutron due to some definite decrease in nuclear excitation is also of importance since the transmission coefficient depends strongly on the neutron kinetic energy.

Candidate daughter levels in ^{178}Hf for neutron acceleration are characterized in Table 2. A minimum orbital angular momentum of the scattered neutron is defined by the spin of the compound nucleus (c. n.), formed from the absorbed

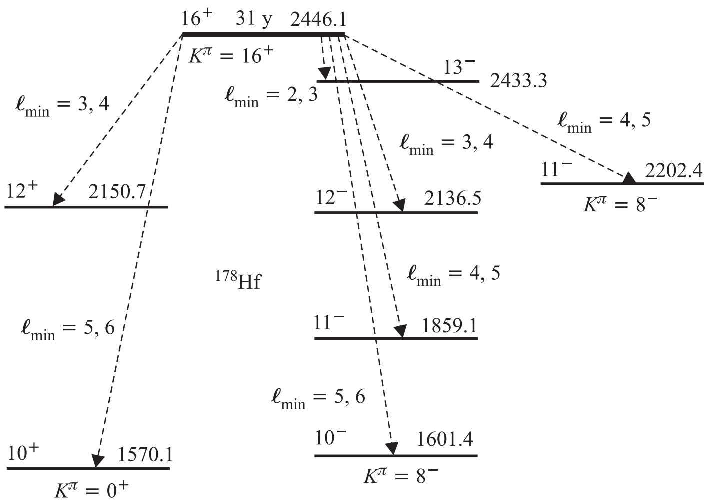

Fig. 3. Levels in ^{178}Hf which may allow inelastic neutron acceleration (superelastic scattering) with the $m2$ isomer as a target. The dashed arrows indicate INNA transitions between the initial isomeric state and specific daughter levels. The $l_{\min}$ values are the minimum orbital angular momenta that must be carried by the accelerated neutron, based on the angular momenta of the compound nucleus reached by the neutron absorption and of the daughter state. As discussed in the text, one $l_{\min}$ value is eliminated for each INNA transition by parity conservation. Level energies are given in keV

neutron and the isomer, and the spin of a specific daughter level. The energy gain of the scattered neutron is simply defined by the difference in initial and final level energies. The parity is even for c. n. resonances formed after slow neutron absorption by the isomer, and neutron emission changes parity as $(-1)^l$. Therefore, neutrons with even l populate even-parity daughter levels and neutrons with odd l populate odd-parity daughter levels: otherwise the population of the daughter level is parity-forbidden. Table 2 lists those initial state (isomer) to final state INNA transitions shown in Fig. 3 which are allowed or prohibited by parity. These restrictions were also recognized in the works [11, 23], although formulated indirectly by expressing that magnetic-type electromagnetic transitions were required from the isomer to the daughter level. It is clear that electric transitions are not forbidden for c. n. resonances with $I_{\text{c.n.}} = (I_m + 1/2)$. Thus, the stated requirement in [11, 23] of magnetic transitions seems misleading not only because of the latter argument, but also because the essence of the INNA process is not inherently bound to the electromagnetic mechanism. Herein, it is preferred to directly reference the role of parity for initial to final state INNA transitions. The nucleus does not undergo electromagnetic transitions from the isomer to a lower-lying daughter level during inelastic neutron acceleration, although the selection rules by parity and angular momentum continue to play a role in neutron emission.

It is clear from Table 2 that, among all possibilities, only the transition from the $31/2^+$ c. n. resonance to the 12^- state with $E_n = 309.6$ keV is favorable for neutron acceleration. This results from the lack of parity hindrance for this transition and a moderate value of T_l for $l = 3$. Other transitions are strongly

Table 2. Predicted level population in the INNA reaction by ^{178}Hf^{m2} ($E^* = 2446.1$ keV, $I^\pi = 16^+$)

Daughter level		Neutron energy gain, keV	Compound nucleus resonance	$l_{\min}$ for accelerated neutron	Hindrance by parity from compound nucleus to daughter
E^*, keV	I^π				
2433.3	13^-	12.7	$31/2^+$	2	Yes
			$33/2^+$	3	No
2202.4	11^-	243.7	$31/2^+$	4	Yes
			$33/2^+$	5	No
2150.7	12^+	295.4	$31/2^+$	3	Yes
			$33/2^+$	4	No
2136.5	12^-	309.6	$31/2^+$	3	No*
			$33/2^+$	4	Yes
1859.1	11^-	586.9	$31/2^+$	4	Yes
			$33/2^+$	5	No

*Most favored daughter level for INNA, due to the moderate value of $l_{\min} = 3$ and lack of parity hindrance.

suppressed either by parity or a negligible T_l. For instance, the transitions from c. n. resonances to the 13^- level with $l = 2$ is forbidden by parity, and with $l = 3$ due to the low energy of the emitted neutron which suppresses T_l. Thus, the theoretical estimate for inelastic neutron acceleration from ^{178}Hf is dominated by this one specific transition having $l = 3$ and $E_n = 309.6$ keV.

The choice of parameters for Eq. (4) used in [11] is consistent with that accepted in neutron physics. Employing those same parameters now for ^{178}Hf, the cross section for inelastic neutron acceleration by this isomer is predicted to be $\sigma_{\rm INNA} = 4$ b, a factor of 7 lower than the theoretical prediction of $\sigma_{\rm INNA} = 27$ b derived [11] for ^{177}Lu^m. In both cases, however, the theoretically calculated cross sections are lower than the measured values by orders of magnitude. The authors of [11] expressed that such a discrepancy may be more or less «plausible», taking into account the statistical nature of theoretically predicted neutron cross sections. The statistical probability distribution was analyzed in [23]. It is difficult to determine at this time whether the observed discrepancies between the experiments and theory are indeed reasonable. For now, the experimental results appear to be more reliable for inelastic neutron acceleration by interactions with isomers.

It is useful at this point to compare all known INNA cross sections, collected in Table 3. Despite the failure of theoretical calculations to explain most of the experimental values, the measurements themselves suggest that relatively high cross sections may be characteristic in the $A \sim 180$ isomer island. The cross section has not yet been measured for any reaction in which the target is the ^{179}Hf^{m2} isomer ($T_{1/2} = 25.1$ d), but its value predicted by Eq. (6) is comparable to that calculated for ^{177}Lu^m [11] and higher than that predicted for ^{178}Hf^{m2} targets. It is possible that the measured cross section for INNA by ^{179}Hf^{m2} may reach the scale of hundreds of barns, if the predicted value is underestimated, the same as for ^{177}Lu^m and ^{178}Hf^{m2}.

Table 3. Comparison of measured and calculated cross sections for parity-allowed INNA reactions

Target isomer	INNA transition	Neutron energy gain, keV	$l_{\rm min}$ for accelerated neutron	$\sigma_{\rm theor}$, b	$\sigma_{\rm exp}$, b	Ref.
^{152}Eu^m	$0^- \to 3^-$	45.6	2	0.3	0.23	[5]
^{177}Lu^m	$23/2^- \to 17/2^-$	125.3*	2	27	258	[11]
^{178}Hf^{m2}	$16^+ \to 12^-$	309.6	3	4	152	Present
^{179}Hf^{m2}	$25/2^- \to 21/2^+$	21.1	1	~ 30	—	Present
^{180}Hf^m	$8^- \to 6^+$	500.7*	1	300	52	[6]

*Transition likely to contribute most INNA cross section due to lowest $l_{\rm min}$ among available levels.

SUMMARY

The K-hindered, 4-quasiparticle isomer $^{178}\mathrm{Hf}^{m2}$ has been the subject of considerable interest and study, due to its nuclear structure and yrast nature. Now, the cross section for inelastic acceleration of thermal neutrons by this isomer has been measured, yielding a value of $\sigma_{\mathrm{INNA}} = 152^{+51}_{-36}$ b. This comprises more than 60% of the total cross section for burn-up of this isomer. The measured cross section for neutron acceleration by this isomer was compared to a theoretical prediction and found to be much larger, in agreement with the results obtained elsewhere for neutron acceleration by $^{177}\mathrm{Lu}^{m}$. INNA represents a somewhat exotic process, which should be studied further with the aim of reconciling experimental and theoretical values for the cases of the Lu and Hf isomers discussed here and for other isomers. At the moment, one may conclude that the INNA reaction supplies a high cross section for isomer depletion, that K-hindrance does not suppress the process, and that parity selection rules restrict the choice of effective daughter levels for INNA. One may expect an even higher yield of the process if the $^{179}\mathrm{Hf}^{m2}$ isomer is taken as a target.

Acknowledgements. The results presented herein are the product of new analysis of the cross sections reported in [12] and the co-authors of that work are gratefully acknowledged for their efforts during those experiments, performed in 2003–2005. The authors acknowledge support by DTRA under contract HDTRA1-08-1-0014.

REFERENCES

1. *Petrov Y. V.* // JETP. 1959. V. 37. P. 1170.
2. *Anandan J., Hagen C. R.* // Phys. Rev. A. 1994. V. 50. P. 2860.
3. *Hammermesh B.* // Phys. Rev. C. 1974. V. 10. P. 2397.
4. *Miyano K., Morinaga H.* // J. Phys. Soc. Japan. 1969. V. 26. P. 576.
5. *Kondurov I. A., Korotkikh E. M., Petrov Yu. V.* // JETP Lett. 1980. V. 31. P. 232.
6. *Kondurov I. A. et al.* // Phys. Lett. B. 1981. V. 106. P. 383.
7. *Brown J. A. et al.* // Phys. Rev. C. 1995. V. 51. P. 1312.
8. *Carroll J. J. et al.* // Hyperfine Int. 2001. V. 135. P. 3.
9. *Karamian S. A.* // Phys. Part. Nucl. 2008. V. 39. P. 950 (in Russian).
10. *Hartouni E. P. et al.* Theoretical Assessment of ^{178m2}Hf Deexcitation. Report LLNL-TR-407631, 2008 (unpublished).

11. *Roig O. et al.* // Phys. Rev. C. 2006. V. 74. P. 054604.

12. *Karamian S. A. et al.* // High Energy Density Phys. 2006. V. 2. P. 48.

13. *Bélier G. et al.* // Phys. Rev. C. 2006. V. 73. P. 014603.

14. *Oganessian Yu. Ts. et al.* // JINR Rapid Comm. 3(54), 72 (1992).

15. *Karamian S. A. et al.* // VI International School-Seminar on Heavy-Ion Physics. Singapore: World Scientific, 1998. P. 565.

16. *Huizenga J. R., Vandenbosch R.* // Phys. Rev. 1960. V. 120. P. 1305.

17. *Karamian S. A. et al.* // Z. Phys. A. 1996. V. 356. P. 23.

18. *Baglin C. M.* // Nucl. Data Sheets. 2009. V. 110. P. 265.

19. *Mullins S. M. et al.* // Phys Rev. C. 2000. V. 61. P. 044315.

20. *Gilbert A., Cameron A. G. W.* // Can. J. Phys. 1965. V. 43. P. 1446.

21. *Karamian S. A. et al.* // Phys. Rev. C. 1999. V. 59. P. 755.

22. *Oganessian Yu. Ts., Karamian S. A.* // Hyperfine Inter. 1997. V. 107. P. 43.

23. *Petrov Yu. V., Shlyakhter A. I.* // Nucl. Sci. Eng. 1981. V. 77. P. 157.

24. *Browne E.* // Nucl. Data Sheets. 1994. V. 72. P. 221.

Received on November 27, 2009.

Корректор *Т. Е. Попеко*

Подписано в печать 24.02.2010.
Формат $60 \times 90/16$. Бумага офсетная. Печать офсетная.
Усл. печ. л. 1,18. Уч.-изд. л. 1,59. Тираж 290 экз. Заказ № 56902.

Издательский отдел Объединенного института ядерных исследований
141980, г. Дубна, Московская обл., ул. Жолио-Кюри, 6.
E-mail: publish@jinr.ru
www.jinr.ru/publish/